

## Surface Pinning and Grain Boundary Formation in Magnetic Flux-Line Lattices of $\text{Bi}_2\text{Sr}_2\text{CaCu}_2\text{O}_{8+\delta}$ High- $T_c$ Superconductors

Hongjie Dai, Jie Liu, and Charles M. Lieber

*Harvard University, Cambridge, Massachusetts 02138*

(Received 18 October 1993)

Magnetic decoration has been used to investigate the role of surface pinning on the flux-line lattice (FLL) of high-quality  $\text{Bi}_2\text{Sr}_2\text{CaCu}_2\text{O}_{8+\delta}$  single crystals. We find that surface steps pin flux lines at the sample surface, and that strong pinning along large steps creates grain boundaries (GBs) in the FLL. Analysis of the competing energetics of pinning versus GB formation leads to a criterion for the formation of extended GBs, and also indicates that these GBs penetrate through the entire sample. Surface pinning, which should occur in all real samples, will thus significantly affect the bulk FLL structure in these materials.

PACS numbers: 74.60.Ge, 74.72.Hs

Understanding the structure, pinning, and dynamics of the magnetic flux-line lattice (FLL) in the copper oxide superconductors is a problem of great fundamental and practical importance [1,2]. Essential information addressing the macroscopic structure of the FLL has come from Bitter patterns in which the positions of individual flux lines at the surface of a superconducting sample are decorated with magnetic particles [3–8]. These experiments, which have illuminated a number of complex FLL structures, have stimulated considerable discussion regarding the  $H$ - $T$  phase diagram and FLL pinning in the copper oxide materials [1,9–12]. In general, it has been assumed that the surface FLL structure produced by decoration is representative of the bulk FLL. There are, however, reasons why this assumption may not be true. For example, since the line tension,  $\epsilon_L \propto (\phi_0/4\pi\lambda)^2 \ln \kappa$ , is significant for the copper oxide materials ( $\approx 100$  K/Å for  $\text{Bi}_2\text{Sr}_2\text{CaCu}_2\text{O}_8$ ) it is possible that surface roughness may strongly pin flux lines as they emerge from the sample surface [9]. A clear understanding of surface effects is thus important to the interpretation of Bitter patterns in terms of bulk FLL structure, and to the analysis of bulk measurements (e.g., small angle neutron scattering) of the FLL.

To this end we have carried out careful studies of surface pinning in Bitter patterns produced by decorating very high-quality  $\text{Bi}_2\text{Sr}_2\text{CaCu}_2\text{O}_{8+\delta}$  (BSCCO) single crystals. Significantly, we find that surface steps pin flux lines at the sample surface, and that strong pinning along large steps creates grain boundaries (GBs) in the FLL. The orientational correlation length extrapolated from measurements within single grains is very long ranged, but because adjacent grains are uncorrelated, the average correlation length is limited by the separation between GBs. In addition, analysis of the competing energetics of pinning versus GB formation leads to a criterion for the formation of extended GBs, and indicates that these GBs penetrate through the samples.

Single crystals of BSCCO were grown using methods described previously [13]. Prior to decoration these crystals were extensively annealed (450°C, 10 d) to remove

oxygen vacancies and extrinsic strain. The transition widths of the annealed BSCCO crystals were typically  $\leq 2$  K, and are indicative homogeneous samples. The crystals were cleaved, and then cooled to 4.2 K in a field parallel to the  $c$  axis prior to decoration. The procedures for decoration and subsequent image analysis have been described previously [3,4,14]. All of the decorations were carried out at 4.2 K.

The central results of our study can be obtained from an analysis of Bitter patterns such as those shown in Fig. 1. First, this image exhibits a large surface step that curves significantly as it crosses the surface. Second, large surface steps, which are observed on all of our crystals regardless of how they are cleaved, strongly pin flux lines. We also note that pinning appears to be asymmetric (i.e., flux lines on the upper and lower terraces interact differently with the step edge). Third, we find that GBs, which extend for large distances ( $\geq 100a_0$ ) in the FLL, originate reproducibly from the edges of large surface steps. Qualitatively, the lattice near the step is bent in response to the pinning potential, but at larger distances an ordered hexagonal lattice is favored. To connect these two boundary conditions necessitates the formation of a GB. We discuss these observations in more detail below.

First, GBs are observed frequently in Bitter patterns of the FLL in high-quality BSCCO samples [15]. The angle between  $G1$  and  $G2$  in Fig. 1(b) is about 26°. Six other GBs with angles ranging from 5° to 32° are shown in a mosaic of images containing  $\approx 12000$  flux lines (Fig. 2). While not shown in this image, the GBs also originate from defects (e.g., surface steps) where flux lines are strongly pinned. In all cases, the FLL is well ordered on either side of a GB with lattice disorder concentrated to within  $\sim 1$  lattice constant of a GB. Qualitatively, these results suggest that surface pinning breaks up the FLL into a polycrystalline structure with randomly oriented grains.

To analyze the GB structure and correlations of the FLL we have carried out Delaunay triangulations of the Bitter patterns using standard methods [3,4,14]. In the

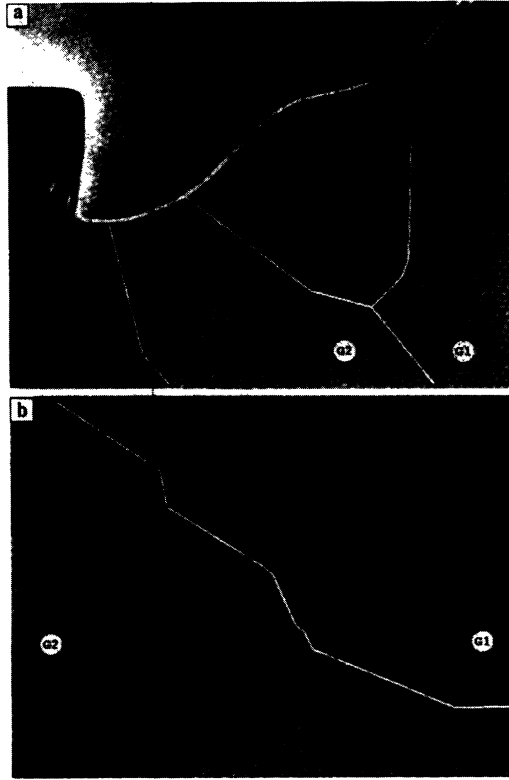


FIG. 1. Bitter pattern of the FLL recorded with a field of 27 G applied perpendicular to the  $a$ - $b$  plane of a BSCCO single crystal. The light spots corresponds to the positions of the flux lines at the surface; the lattice constant is  $\sim 0.95 \mu\text{m}$ . A large, curving surface is present in (a). By viewing the image at a glancing angle along the step it is readily apparent that the flux lines are strongly pinned to this step. GBs which originate from the surface step are highlighted with white lines. The pattern in (b) corresponds to the FLL  $\sim 50$  lattice constants below the lower right of (a), where the BG separating grains 1 and 2 ( $G1, G2$ ) continues from (a) through (b).

Delaunay triangulation a flux line corresponds to the vertex formed by "bonds" between the flux line and its  $n$ -nearest neighbors. Shaded topological defects (i.e., non-sixfold coordinate flux lines) clearly highlight the six GBs in Fig. 2. These defects consist of alternating five-coordinate/seven-coordinate lattice sites running along the direction of the GB. Because of this alternation, the stress-strain fields generated by the defects approximately cancel each other. This arrangement of defects explains why strong lattice disorder is localized to within  $\approx 1$  lattice constant ( $a_0$ ) of the GB [16]. Between GBs the FLL is well ordered and appears unaffected by surface pinning. We thus believe that the FLL within individualized grains is representative of the bulk structure. Notably, the orientational correlation length extrapolated from measurements made within the single grain of Fig. 2 is on the order of the sample size [17]. Because adjacent grains are uncorrelated, the average orientational correlation length corresponds to the average GB spacing.

We believe a more significant finding of our study comes from an analysis of the relative energetics of pinning versus GB formation. For a surface step of height  $s$  and linear dimension  $L'$ , the step pinning energy  $E_p$  is

$$E_p = \epsilon_L s n_0 L' a_0, \quad (1)$$

where  $\epsilon_L$  is the line tension defined earlier and  $n_0$  is the areal vortex density. To estimate the energy of the FLL GB requires an estimate of how far the stress-strain field of dislocations penetrates perpendicular (along the  $c$  axis) to the plane of surface image [18,19]; we define this constant  $l_{c\parallel}$ . The energy of a grain boundary  $E_{GB}$  of angle  $\theta$  and length  $L$  can be written

$$E_{GB} = \epsilon_0 L l_{c\parallel}. \quad (2)$$

The energy per unit area of the GB penetrating into the sample,  $\epsilon_0$ , is

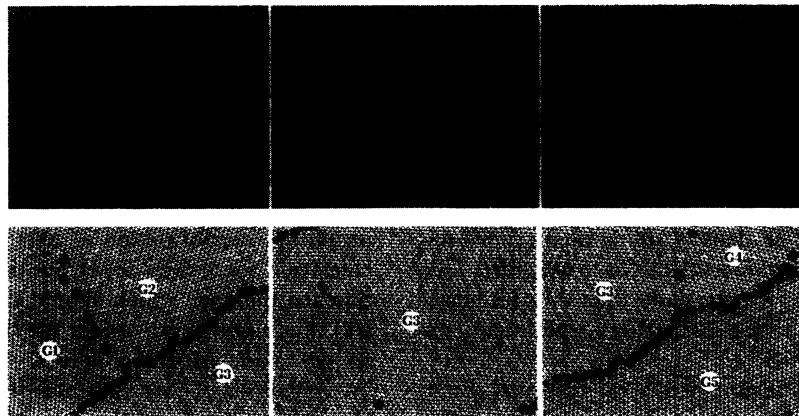


FIG. 2. Upper panels: Mosaic of three nearly adjacent flux-line images recorded in a field of 18 G applied perpendicular to the BSCCO  $a$ - $b$  plane; the images contain  $\sim 12000$  flux lines. The images contain six GBs. Lower panels: Delaunay triangulation of the upper experimental images. Topological defects (nonsixfold flux lines) are indicated by shading. The shaded bands in these images correspond to GBs that separate FLL grains  $G1$ - $G5$ . The GB angle between  $G1/G2$ ,  $G1/G3$ ,  $G2/G3$ ,  $G3/G4$ ,  $G3/G5$ , and  $G4/G5$  are  $13^\circ$ ,  $32^\circ$ ,  $20^\circ$ ,  $6^\circ$ ,  $27^\circ$ , and  $32^\circ$ , respectively. The lattice constant is  $\sim 1.2 \mu\text{m}$ .

$$\varepsilon_0 = \frac{\mu b}{4\pi} \theta \ln \frac{1}{\theta}, \quad (3)$$

where the Burgers vector  $b \approx a_0$  and  $\mu$  is the FLL elasticity [19]. At low fields corresponding to our experiments  $\mu \approx 4C_{66} \approx \phi_0 B / 16\pi^2 \lambda^2$ . To observe GB formation it is expected that  $E_p \geq E_{GB}$ , and thus by combining (1)–(3) we obtain the condition

$$s_c \geq \alpha \frac{L}{L'}, l_{c\parallel}, \quad (4)$$

where  $s_c$  is the critical step height necessary for GB formation and  $\alpha = \theta \ln(1/\theta) / 4\pi \ln \kappa$ .

The physics in Eq. (4) are simple but informative. First, there is a critical step height  $s_c$  necessary for GB formation. Second,  $s_c$  depends purely on surface roughness and is independent of magnetic field. This prediction is consistent with our data since GBs are always observed in Bitter patterns for  $10 < B < 100$  G. Third, one can also estimate a critical step height using reasonable parameters. Analysis of images such as Fig. 1 indicates that  $L'$  and  $L$  are of the same order of magnitude ( $\approx 100 \mu\text{m}$ ). Because a dislocation line cannot end within a crystal, it must either (1) pass through the entire sample, (2) exit the side of the sample, or (3) loop and exit the top of the sample. We believe, however, that explanations (2) and (3) are unlikely.

Hence, assuming that dislocations pass straight through the sample implies that the crystal thickness  $l_{c\parallel} \approx 20 \mu\text{m}$  (typical for our experiments). Substitution into Eq. (4) then yields  $s_c \geq 1000 \text{ \AA}$ . Notably, direct measurements of the heights of the large steps on BSCCO by atomic force microscopy (AFM) demonstrate that they are typically within the 500–1000  $\text{\AA}$  range [20]. These results suggest that very large surface roughness, on the order of 50–100 unit cells, is needed to induce the formation of GBs. Alternatively, one can assume that the dislocation lines penetrate only a short distance into the sample [e.g., case (2) or (3) above] such that roughness on the order of a single unit cell is sufficient to lead to GB formation. Our experimental data appear to rule out this latter possibility (Fig. 3). For example, small surface steps with heights on the order of 1–2 unit cells running across Fig. 3 do not create GBs (the absence of GBs is readily seen by sighting down FLL rows at a glancing angle). Flux lines are pinned to these steps as evidenced by local disorder and higher density along steps; however, this pinning energy is insufficient to form extended GBs in the FLL. Therefore, we conclude that the GB structures observed in our surface decoration experiments extend through the bulk FLL.

These results are significant in several respects. First, they clearly show that surface roughness can pin the flux lines imaged by the decoration technique. Second, while it has been argued that Bitter patterns may not represent bulk FLL structure in the presence of pinning by surface roughness, our result demonstrates a significant twist:

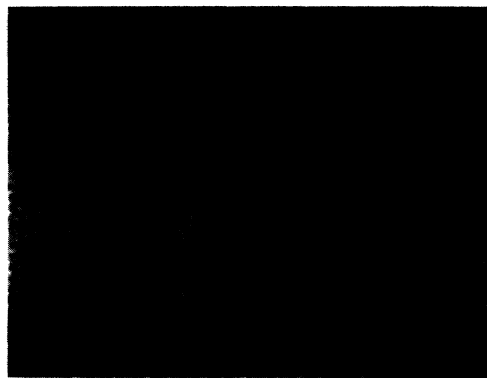


FIG. 3. Bitter pattern recorded in a field of 27 G applied perpendicular to the BSCCO  $a$ - $b$  plane. Several small surface steps run across the middle of this image and are highlighted with white arrows. The flux-line density along these steps is higher than the average spacing for this field. The lattice constant is  $\sim 0.95 \mu\text{m}$ .

Surface steps exceeding a critical height (which depends on sample thickness) create GBs that extend through the bulk of the FLL. Hence, for real samples (i.e., with surface roughness and finite size) we expect that surface pinning (detected in decoration experiments) can have a very significant influence on the bulk state. Between BGs, however, we believe that the surface FLL is representative of the bulk. Our results are also important in light of recent neutron scattering studies of BSCCO [21]. In these experiments, which probe bulk FLL structure, it was found that the scattering peaks had tangential widths on the order of  $35^\circ$ . The decoration images (Figs. 1 and 2) show that the FLL has a polycrystalline structure with GBs up to  $\approx 30^\circ$ , and thus scattering from these uncorrelated grains will yield large tangential widths in the bulk neutron measurements. The important point is that this could arise from a purely surface or finite size effect.

In conclusion, we have used magnetic decoration to study the role of surface pinning on the FLL in high-quality BSCCO single crystals. Significantly, we find that surface steps pin flux lines at the sample surface, and that strong pinning along large steps creates grain boundaries (GBs) in the FLL. Analysis of the competing energetics of pinning versus GB formation leads to a criterion for the formation of extended GBs, and also indicates that these GBs penetrate through the entire sample. Surface pinning, which should occur in all real samples, will thus significantly affect the bulk FLL structure in the copper oxide superconductors. We believe that further investigations of these surface derived extended defects is clearly warranted.

The authors would like to thank P. Gammel for his generous advice during our initial decoration experiments and D. R. Nelson for critical discussion and helpful suggestions. C.M.L. acknowledges support of this work by

NSF (DMR 9306684).

- 
- [1] D. J. Bishop, P. L. Gammel, D. A. Huse, and C. A. Murray, *Science* **255**, 165 (1992).
- [2] D. A. Huse, M. P. A. Fisher, and D. S. Fisher, *Nature (London)* **358**, 553 (1992).
- [3] C. A. Bolle, P. L. Gammel, D. G. Grier, C. A. Murray, D. J. Bishop, D. B. Mitzi, and A. Kapitulnik, *Phys. Rev. Lett.* **66**, 112 (1991).
- [4] D. G. Grier, C. A. Murray, C. A. Bolle, P. L. Gammel, D. J. Bishop, D. B. Mitzi, and A. Kapitulnik, *Phys. Rev. Lett.* **66**, 2270 (1991).
- [5] G. J. Dolan, G. V. Chandrashekhar, T. R. Dinger, C. Feild, and F. Holtzberg, *Phys. Rev. Lett.* **62**, 827 (1989).
- [6] P. L. Gammel, C. A. Durán, D. J. Bishop, V. G. Kogan, M. Ledvij, A. Yu. Simonov, J. P. Rice, and D. M. Ginsberg, *Phys. Rev. Lett.* **69**, 3808 (1992).
- [7] P. L. Gammel, D. J. Bishop, J. P. Rice, and D. M. Ginsberg, *Phys. Rev. Lett.* **68**, 3343 (1992).
- [8] I. V. Grigorieva, K. E. Bagnall, P. A. Midgley, K. Sasaki, and J. W. Steeds, *Physica (Amsterdam)* **199C**, 73 (1992).
- [9] D. A. Huse, *Phys. Rev. B* **46**, 8621 (1992).
- [10] D. S. Fisher, M. P. A. Fisher, and D. A. Huse, *Phys. Rev. B* **43**, 130 (1991).
- [11] M. C. Marchetti and D. R. Nelson, *Phys. Rev. B* **47**, 12214 (1993).
- [12] M. C. Marchetti and D. R. Nelson, *Phys. Rev. B* **41**, 1910 (1990).
- [13] Y. Li, J. Liu, and C. M. Lieber, *Phys. Rev. Lett.* **70**, 3494 (1993).
- [14] H. Dai and C. M. Lieber, *Phys. Rev. Lett.* **69**, 1576 (1992).
- [15] In samples containing point defects such as oxygen vacancies, disorder in FLL caused by collective pinning may obscure GBs.
- [16] In the lower angle grain boundaries found in upper left and right sides of Fig. 2 the dislocations as expected are not closely paired. For these small angle GBs it is possible to use classical theory [19] to estimate the distance  $D$  between dislocations:  $D = a_0/2 \sin(\theta/2)$ . For  $\theta = 13^\circ$  (upper left GB)  $D \approx 4.5a_0$ , and for  $\theta = 5^\circ$  (upper right)  $D \approx 11a_0$ , in agreement with our data.
- [17] A fit of the orientational correlation function  $[G_6(r)]$  by an exponential decay,  $G_6(r) \propto \exp(-r/\epsilon_6)$ , yields a correlation length of  $\sim 980a_0$ . Notably, this corresponds to the dimension of the sample,  $\sim 1$  mm. However,  $G_6(r)$  drops essentially to zero upon crossing a GB, and thus the GB spacing defines the orientational correlation length.
- [18] W. T. Read and W. Shockley, *Phys. Rev.* **78**, 275 (1950).
- [19] F. N. R. Nabarro, *Theory of Crystal Dislocations* (Dover, New York, 1987).
- [20] S. Yoon, H. Dai, and C. M. Lieber (unpublished).
- [21] R. Cubitt, E. M. Forgan, G. Yang, S. L. Lee, D. McK. Paul, H. A. Mook, M. Yethiraj, P. H. Kes, T. W. Li, A. A. Menovsky, Z. Tarnawski, and K. Mortensen, *Nature (London)* **365**, 407 (1993).

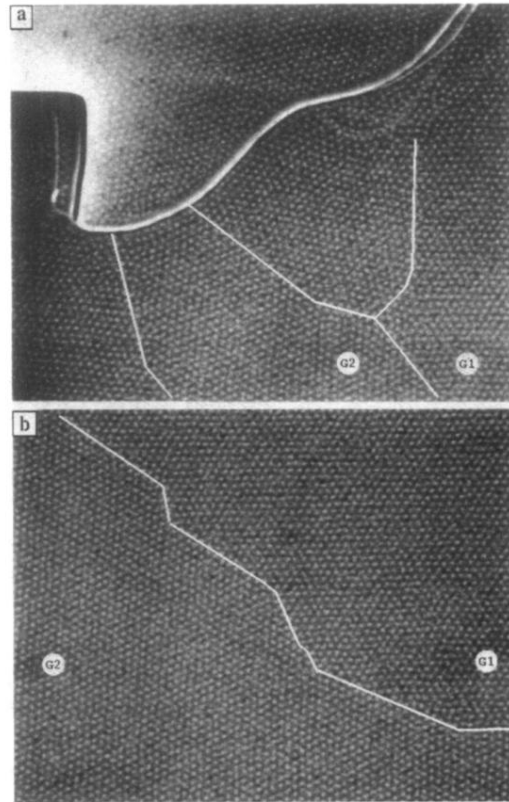


FIG. 1. Bitter pattern of the FLL recorded with a field of 27 G applied perpendicular to the  $a$ - $b$  plane of a BSCCO single crystal. The light spots corresponds to the positions of the flux lines at the surface; the lattice constant is  $\sim 0.95 \mu\text{m}$ . A large, curving surface is present in (a). By viewing the image at a glancing angle along the step it is readily apparent that the flux lines are strongly pinned to this step. GBs which originate from the surface step are highlighted with white lines. The pattern in (b) corresponds to the FLL  $\sim 50$  lattice constants below the lower right of (a), where the BG separating grains 1 and 2 ( $G1, G2$ ) continues from (a) through (b).

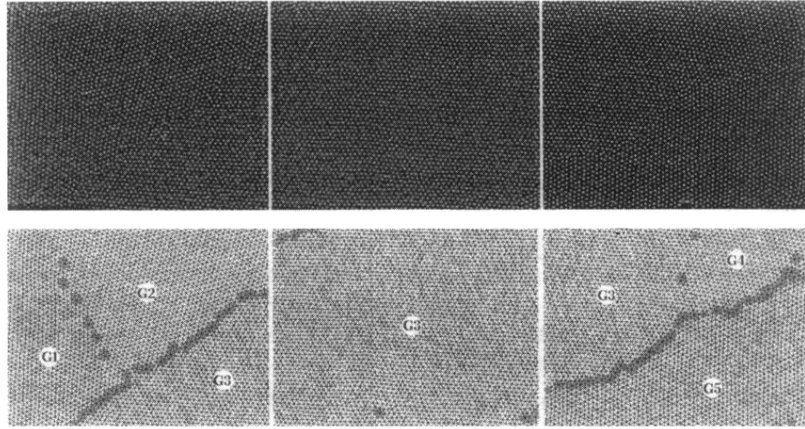


FIG. 2. Upper panels: Mosaic of three nearly adjacent flux-line images recorded in a field of 18 G applied perpendicular to the BSCCO  $a$ - $b$  plane; the images contain  $\sim 12000$  flux lines. The images contain six GBs. Lower panels: Delaunay triangulation of the upper experimental images. Topological defects (nonsixfold flux lines) are indicated by shading. The shaded bands in these images correspond to GBs that separate FLL grains  $G1$ - $G5$ . The GB angle between  $G1/G2$ ,  $G1/G3$ ,  $G2/G3$ ,  $G3/G4$ ,  $G3/G5$ , and  $G4/G5$  are  $13^\circ$ ,  $32^\circ$ ,  $20^\circ$ ,  $6^\circ$ ,  $27^\circ$ , and  $32^\circ$ , respectively. The lattice constant is  $\sim 1.2 \mu\text{m}$ .

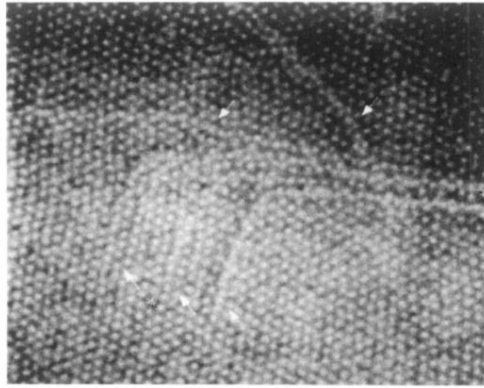


FIG. 3. Bitter pattern recorded in a field of 27 G applied perpendicular to the BSCCO  $a$ - $b$  plane. Several small surface steps run across the middle of this image and are highlighted with white arrows. The flux-line density along these steps is higher than the average spacing for this field. The lattice constant is  $\sim 0.95 \mu\text{m}$ .